Fabrication of wurtzite ZnS nanobelts via simple thermal evaporation

Quan Li[a] and Chunrui Wang
Department of Physics, The Chinese University of Hong Kong, Shatin, New Territory, Hong Kong, China

(Received 2 January 2003; accepted 14 May 2003)

Mass production of uniform wurtzite-ZnS nanobelts is achieved by a simple thermal evaporation method using Au as the catalyst. The as-synthesized ZnS nanobelts are single crystalline, usually several tens of microns in length and several hundreds of nanometers in width. Most of the nanobelts grow along [01 1 0] direction. Stacking faults are commonly observed in these nanobelts. The room-temperature cathodoluminescence spectrum of such nanobelts reveals three peaks, which may be ascribed to surface states, defects, and impurity-induced emissions, and is consistent with the nanobelt microstructure. The growth mechanism of the nanobelts is discussed. © *2003 American Institute of Physics.* [DOI: 10.1063/1.1591999]

ZnS, with a band gap of 3.7 eV (at 300 K), is a promising material for optoelectronic applications in the near-ultraviolet spectral region. It has a large exciton binding energy (40 meV) and a small Bohr radius (2.4 nm), which makes it an excellent candidate in exploring the intrinsic recombination processes in dense excitonic system. Transition-metal or rare-earth-element-doped ZnS has been used as effective phosphor material for a long time,[1] and the luminescence property of both bulk and nanocrystalline ZnS[2] is an area of great interest due to its potential technological applications. Controlling the size and the dimensionality of ZnS crystals may further lead to novel properties due to the quantum confinement effect. Recently, one-dimensional (1D) growth the ZnS-based nanostructures have been reported, including ZnS nanowire growth by liquid crystal template,[3] micelle-template,[4] thermal evaporation using Au catalyst,[5] and ZnO–ZnS nanocable, and ZnS nanotube synthesized via ZnO nanobelts template.[6] Another interesting configuration of the 1D growth is nanobelts, in which the thickness of the belt is much smaller than its width, so that the confinement is far from uniform in the cross section compared to its nanowire counterparts. In this work, we report the mass production of uniform ZnS nanobelts by a simple way of thermal evaporation with Au as the catalyst. Stacking faults with fault planes parallel to the nanobelt growth direction are commonly observed in these nanostructures. Room-temperature cathodoluminescence (CL) measurement of the as-deposited sample reveals three peaks, which can be related to surface states and impurity-related emissions. The growth mechanisms of such nanobelts are discussed.

The fabrication process is based on thermal evaporation of ZnS powders in the presence of Au catalyst. An alumina tube was mounted horizontally inside a high-temperature tube furnace. Two grams of ZnS powder (99.99% ARCO) were placed in the center of the tube. Silicon wafers were first sputter-coated with a layer of gold thin film (~5 nm), and then placed downstream in the tube. The tube was then pumped down to a base pressure of 2×10^{-2} Torr. The furnace was heated up to 1200 °C for 2 h before being cooled down to room temperature. During the fabrication process, a constant flow of Ar was introduced in the tube at a flow rate of 100 sccm. The deposition pressure was kept at 300 mTorr. The general morphology of the products was examined by secondary electron microscopy (SEM, LEO 1450VP). Powder x-ray diffraction (XRD, Rigakau RU-300 with Cu K_{α_1} radiation) was employed to examine their overall crystallinity. Detailed microstructure analysis was carried using transmission electron microscopy (TEM) with a Philips CM 120 microscope operating at 120 kV. The chemical composition analysis was achieved by energy dispersive x-ray spectrometry (EDX), using an EDX spectrometer attached to the same microscope. The room-temperature CL study of the nanobelts was carried by a MonoCL system (Oxford Instrument) in a scanning electron microscope. The accelerating voltage was kept at 20 kV, and the excitation power was kept at 20 μW to minimize the radiation damage induced by the electron beam.

Figure 1 shows a SEM image of the as-deposited products on the Au-coated silicon substrate. The products consist of large quantity of wire-like nanostructures with typical length in the range of several tens of microns, and width several hundreds of nanometers. A higher magnification image in the upper-right inset shows several twisted ''wires,'' displaying the shape characteristic of a nanobelt. It is also observed that the nanobelts are almost electron transparent, which further suggests that the thickness of these nanobelts is small. A powder XRD pattern of such nanobelts is shown in Fig. 2. All of the diffraction peaks can be indexed to those of the wurtzite ZnS (hexagonal) with lattice constant $a=3.822$ Å and $c=6.260$ Å (JCPDS) within the experimental error.

Detailed microstructure information and chemical composition of individual nanobelts are obtained through TEM studies. Figure 3(a) shows the general morphology of the nanobelts, which are dispersed on the carbon film. They are relatively uniform, with widths in the range of hundreds of nanometers, which is consistent with the SEM observations. Their side surfaces are not smooth. An EDX spectrum of the nanobelts indicates that they consist of Zn and S only [Fig. 3(b)]. These nanobelts appear to be brittle; many of them break in the middle during the TEM sample preparation pro-

[a]Author to whom correspondence should be addressed; electronic mail: liquan@phy.cuhk.edu.hk

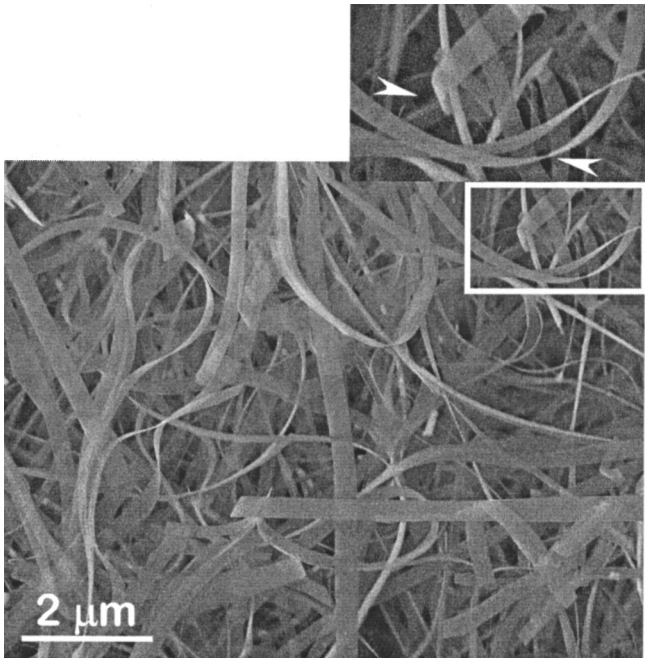

FIG. 1. SEM image of the products on silicon substrate, revealing a belt-like feature.

cess and leave a sharp edge at the end of the nanobelt [marked by an arrow in Fig. 3(a)]. Nevertheless, particle-like materials are found at one end of some of the nanobelts. The particle appears to be dark, suggesting a larger mass-thickness value compared to the ZnS [Fig. 3(c)]. The size of the particle is smaller than the width of the ZnS nanobelt, usually in the range of ≃100 nm. EDX spectrum taken from the particle indicates that it is composed of Au [Fig. 3(d)].

Although stacking fault-free nanobelts are observed, many of them are heavily faulted (~1/3 across the belt width). Stacking faults along the belt growth direction are the most commonly observed defect in these nanobelts. A typical example is shown in Fig. 4, where lines of stacking faults [(0002) planes] are parallel to the nanobelt axial direction. The transmission electron diffraction (TED) pattern of the same nanobelt is shown in the inset of Fig. 4. It can be indexed to the hexagonal ZnS $\langle 2\,\bar{1}\,1\,0\rangle$ zone axis. Out-of-focus diffraction indicates that the nanobelt grows along

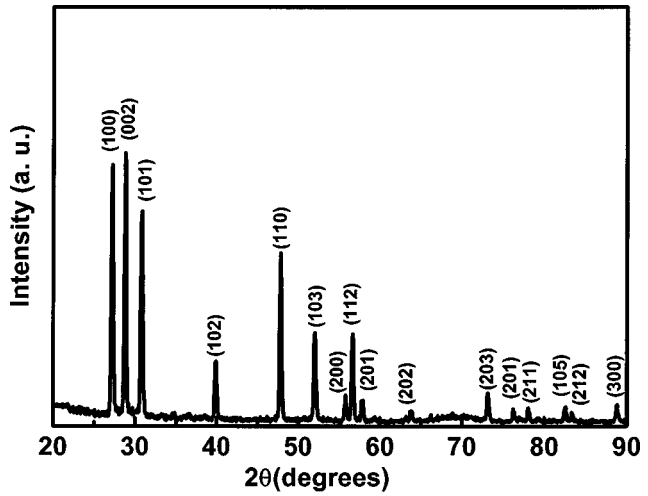

FIG. 2. XRD of the products shown in Fig. 1.

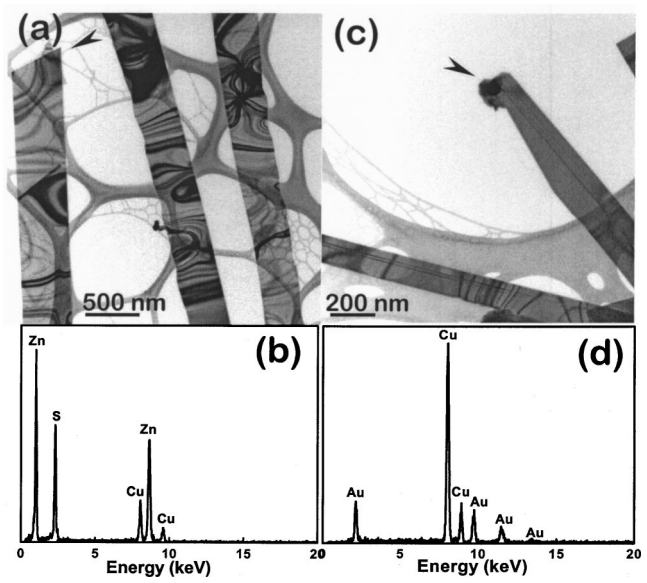

FIG. 3. (a) Bright-field TEM image of several ZnS nanobelts; (b) EDS of the nanobelts shown in Fig. 3(a); (c) Bright-field image of a nanobelt with a dark tip; (d) EDS taken from the tip area.

$[01\,\bar{1}\,0]$ direction. The spike extended from each diffraction spot results from the stacking faults, which is consistent with those observed in Fig. 4. TED investigation of several tens of nanobelts indicates that they universally grown along $[01\,\bar{1}\,0]$ direction.

The room-temperature CL spectrum of such nanobelts is shown in Fig. 5. Three broad emission peaks at different photon energies are detected. They are located at 3.47, 2.73, and 2.30 eV, respectively.

The formation of the ZnS nanobelts may relate to the vapor–liquid–solid (VLS) mechanism,[7] where Au liquid droplets serve as the preferential absorption site for the nanobelts. Several experimental observations support this conclusion: (1) Although Au film is used in the experiment, it splits into small Au liquid droplets at elevated temperatures.[8] Al-

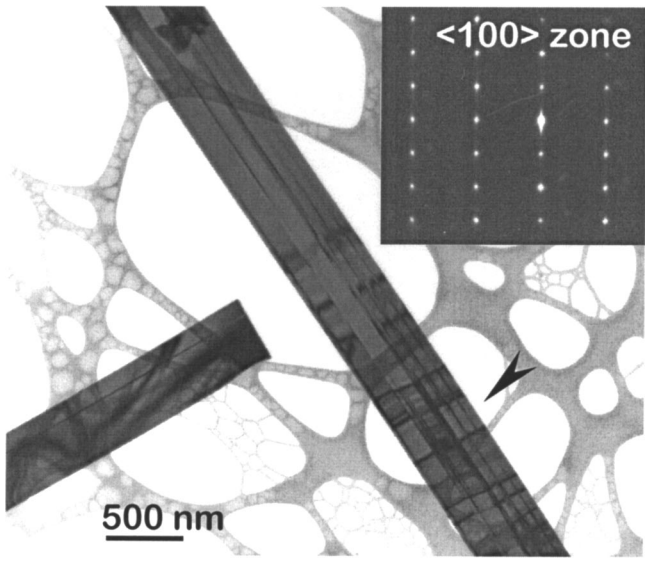

FIG. 4. Bright-field image of one nanobelt with stacking fault planes along the belt growth direction. The diffraction in the inset indicates that the belt grows along $[0\bar{1}10]$ direction, and the spike at each diffraction spot suggests the existence of stacking faults.

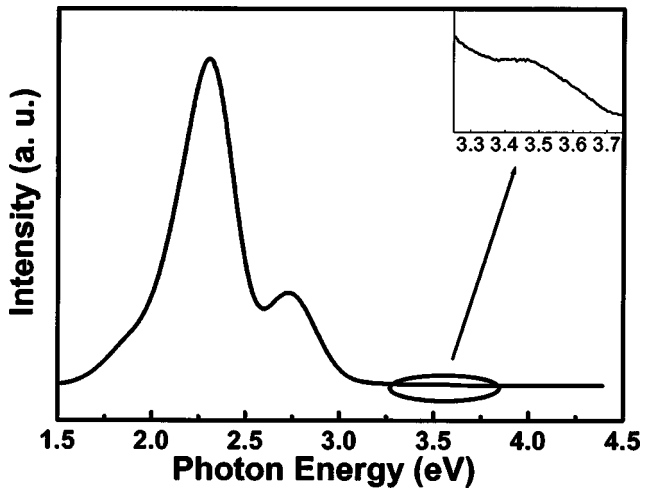

FIG. 5. Room-temperature CL spectrum of the as-synthesized ZnS nanobelts, revealing three broad peaks centered at 3.47, 2.73, and 2.30 eV, respectively.

though the size of the Au droplet depends on the thickness of the film,[8] its minimum size achievable is determined by the thermal equilibrium at specific temperatures, which is in the range of several tens of nanometers to $\simeq$100 nm.[7] This is consistent with the TEM observation of the nanobelt tip size. (2) Thermal evaporation of ZnS powder at the same experimental condition but in the absence of Au results in large ZnS whiskers with little yield on the Si substrate, but mainly on the tube walls. This suggests that the vapor phase containing Zn and S is preferentially accommodated by the liquid Au catalyst due to its large accommodation coefficient.[7] Nevertheless, the nanobelts growth process may differ from the conventional VLS mechanism, in which the size of the whisker (or nanowire) is confined by the size of the catalyst particle. In the current study, Au may only be involved during the physical absorption process rather than further contribute to the 1D growth. Obviously, parameters that affect the crystal growth kinetics may play important roles in deciding nanobelt morphology. The fabrication temperature is found to be one of such parameters. For ZnS powder evaporated at lower temperature, only nanowires result. This is consistent with a previous report of the ZnS nanowire growth by Wang *et al.*[6] It was also pointed out by several other researchers during their research of oxide nanowires and nanobelts that the nanobelt growth prefers higher temperature conditions.[9] The frequent observation of tip-to-end stacking faults along the nanobelts growth direction may be due to the fact that the (0002) plane is the most preferable slip plane in hexagonal materials such as ZnS.

The emissions in the CL spectrum can be ascribed to the following mechanisms. The small peak at 3.46 eV may be ascribed to the hole traps originating from unsaturated sp^3 orbitals of surface S atoms,[10] which was suggested by Kumbhojkar *et al.* during their study of ZnS nanoparticles. The observation of such emission peak from the nanobelts reveals the large surface-to-volume ratio in the nanobelt configuration. The peak at 2.74 eV is normally explained by native defect in the ZnS, including vacancies and dislocations.[11] The observation of high defect densities in the nanobelt is consistent with the CL spectrum. The possibility of such an emission peak resulting from Cl impurities[12] can be excluded, as no Cl has been introduced during the experiment. The last emission peak at 2.27 eV was also observed by Wang *et al.* during their synthesis of ZnS nanowires, and is understood as the Au impurity-related deep level emission.[5] Mitsui *et al.* point out such emission may be associated with point defects, which are most likely the isolated Zn vacancy in the single negative charge state.[13]

In conclusion, mass production of uniform ZnS nanobelts is achieved by a simple thermal evaporation method with Au as the catalyst. These nanobelts are several tens of microns in length and several hundreds of nanometers in width. They grow universally along $[0\bar{1}10]$ direction, and are usually heavily faulted. The Au film forms liquid droplets during the fabrication process (at elevated temperatures), which serve as the preferential adsorption sites for Zn and S in the vapor phase. The morphology of ZnS (nanowire or nanobelt) may be decided by the parameters that affect crystal growth kinetics, and the fabrication temperature is recognized to be one of such parameters. The CL spectrum of the as-deposited nanobelts reveal three emission peaks, which can be explained by their increase surface/volume ratio, heavy defect density, and the catalyst impurity.

This research is supported by RGC direct allocation in the Chinese University of Hong Kong, under project No. 2060227.

[1] S. C. Qu, W. H. Zhou, F. Q. Liu, N. F. Chen, Z. G. Wang, H. Y. Pan, and D. P. Yu, Appl. Phys. Lett. **80**, 3605 (2002); L. Cao, J. Zhang, S. Ren, and S. Huang, *ibid.* **80**, 4300 (2002).
[2] M. V. Nazarov, Mater. Sci. Eng., B **91–92**, 349 (2002).
[3] Y. Xie, J. X. Huang, B. Li, and Y. T. Qian, Adv. Mater. (Weinheim, Ger.) **12**, 1523 (2000); X. Jiang, Y. Xie, J. Lu, L. Y. Zhu, W. He, and Y. T. Qian, Chem. Mater. **13**, 1213 (2001).
[4] Q. S. Wu, N. W. Zheng, Y. P. Ding, and Y. D. Li, Inorg. Chem. Comm. **5**, 671 (2002).
[5] Y. W. Wang, L. D. Zhang, C. H. Liang, G. Z. Wang, and X. S. Peng, Chem. Phys. Lett. **357**, 314 (2002).
[6] X. D. Wang, P. X. Gao, J. Li, C. J. Summers, and Z. L. Wang, Adv. Mater. (Weinheim, Ger.) **14**, 1732 (2002).
[7] R. S. Wagner, *Whisker Technology*, edited by A. P. Levitt (Wiley-Interscience, New York, 1970).
[8] M. H. Huang, Y. Y. Wu, H. Feick, N. Tran, E. Weber, and P. D. Yang, Adv. Mater. (Weinheim, Ger.) **13**, 113 (2001).
[9] Z. W. Pan, Z. R. Dai, and Z. L. Wang, Science **291**, 1947 (2001), B. D. Yao, Y. F. Chen, and N. Wang, Appl. Phys. Lett. **81**, 757 (2002).
[10] N. Kumbhojkar, V. V. Nikesh, A. Kshirsagar, and S. Mahamuni, J. Appl. Phys. **88**, 6260 (2000).
[11] N. Murase, R. Jagannathan, Y. Kanematsu, M. Watanabe, A. Kurita, K. Hirata, T. Yazawa, and T. Kushida, J. Phys. Chem. B **103**, 754 (1999).
[12] B. G. Yacobi and D. B. Holt, *Cathodoluminescence microscopy of inorganic solid* (Plenum, New York, 1990).
[13] T. Mitsui, N. Yamamoto, T. Tadokoro, and S. Ohta, J. Appl. Phys. **80**, 6972 (1996).